Exploring the Role of Inverter Based Resources in Unit Commitment and Optimal Dispatch Under High Renewable Penetration Scenarios

Marco Navia[a], Matija Pavičević[b], Sergio Balderrama[c] and Sylvain Quoilin[a]

[a] Université de Liège, Liege, Belgium, manavia@uliege.be
[b] UC Louvain la Neuve, Leuven, Belgium, matija.pavicevic@uclouvain.be
[c] Universidad Mayor de San Simon, Cochabamba, Bolivia, s.balderrama@umss.edu

Abstract:
The rapid transition toward power systems dominated by inverter-based resources (IBR) is reducing synchronous inertia and altering frequency dynamics in ways that challenge conventional operational planning. Existing frequency-constrained UCED formulations often neglect the combined effect of virtual inertia, fast frequency response, and reserve coordination in weakly interconnected systems. This paper proposes a two-stage framework that links a Frequency Response Assessment Model (FRAM) with an open-source Dispa-SET Unit Commitment and Economic Dispatch (UCED) model. FRAM quantifies contingency-driven frequency security requirements for RoCoF, nadir and steady-state frequency, including contributions from virtual inertia (VIR) provided by IBR. These requirements are translated into UCED security constraints and reserve balances for FFR, FCR, aFRR and mFRR. The methodology is applied to the Bolivian power system for 2030 transition scenarios. Results show that IBR-provided frequency services reduce synchronous capacity needs, improve stability margins, and lower dispatch cost while preserving system reliability. The study delivers a reproducible modelling pathway for evaluating frequency stability in low-inertia, high-renewable systems and supports the design of future grid codes for emerging power systems.

Keywords:
Grid-forming inverters, Inverter-based resources, Low-inertia power systems, Frequency stability, Unit Commitment, Economic Dispatch, Frequency services, Virtual inertia, Power system modeling.

1. INTRODUCTION

The increasing penetration of inverter-based resources (IBRs), including wind, photovoltaic, and battery energy storage systems, is reshaping power system operation and the provision of frequency stability services [4, 8]. Traditionally, inertia and primary frequency response were inherently provided by synchronous machines through electromechanical dynamics. As these units are progressively displaced, system inertia declines, leading to faster and deeper frequency excursions following disturbances, particularly in weakly interconnected systems [1, 7]. In contrast, IBRs provide frequency support through control-based mechanisms embedded in power electronic converters, making their contribution dependent on control design and operating conditions rather than intrinsic physical properties.

Advances in converter control have enabled IBRs to contribute to frequency stability through different strategies. Grid-following converters, synchronized via phase-locked loops, provide limited fast response but rely on an external voltage reference, whereas grid-forming approaches can emulate synchronous behavior and actively support frequency through virtual inertia and droop-based response [8, 3]. As a result, frequency services are increasingly defined by configurable control characteristics, and their representation in operational planning models becomes essential. Recent efforts have incorporated frequency-security constraints into unit commitment and economic dispatch (UCED) formulations. Early work such as [10] demonstrated the feasibility of embedding dynamic frequency constraints in unit commitment for isolated systems. Subsequent studies have extended these formulations to systems with high renewable penetration. Gao et al. [2] introduce frequency constraints based on simplified dynamic models, while Xu et al. [9] account for virtual inertia provision from wind generation within a robust UC framework. Panwar et al. [5] propose a learning-based formulation to enforce RoCoF constraints, and She et al. [6] include virtual inertia scheduling in UC models for low-inertia systems.

While these approaches integrate frequency-security considerations into operational planning, they typically rely on aggregated or linearized representations of system dynamics and emphasize instantaneous power-based constraints, such as inertia levels or reserve headroom. As a result, the interaction between multiple frequency services and their associated energy requirements over the full activation period remains only par-

tially represented. Moreover, most implementations are validated on reduced-scale or benchmark systems, with limited evidence of applicability to large-scale or long-term UCED studies representative of national power systems. Consequently, the explicit representation of IBR-based frequency services in large-scale operational planning remains limited, and the operational and economic implications of co-optimizing energy dispatch with services such as virtual inertia and fast frequency response are not yet fully understood.

This work addresses these limitations through a two-stage framework that explicitly links dynamic frequency performance and operational planning. A Frequency Response Assessment Model (FRAM) is first used to determine minimum inertia and frequency response requirements under N-1 contingencies, considering RoCoF, frequency nadir, and steady-state constraints. These requirements are then embedded into a UCED formulation through service-specific reserve participation factors, enabling the co-optimization of energy and multiple frequency services, including virtual inertia. Unlike headroom-based formulations, the proposed approach captures the interaction between services and accounts for both power and energy requirements over the full activation period.

The proposed structure maintains computational tractability by decoupling dynamic assessment from optimization, enabling application to larger systems and longer time horizons. At the same time, it provides flexibility to incorporate more detailed control representations, such as frequency deadbands, damping terms in synthetic inertia emulation, and non-linear droop characteristics.

The remainder of the paper is organized as follows. Section 2 presents the modeling framework and formulations. Section 3 describes the case study. Section 4 discusses the results, and Section 5 concludes the paper.

2. METHODOLOGY

2.1. Technology–Operation Interaction

The proposed framework establishes an open-loop interaction between system dynamics and operational decision-making through three sequential stages. First, a preliminary UCED simulation is performed without frequency security constraints to obtain dispatch schedules and system operating conditions. Second, the FRAM model is applied offline to the hourly operating profiles and representative contingencies obtained from the preliminary UCED simulation to quantify system-wide frequency response requirements, including inertia and reserve needs. These requirements are subsequently stored and passed to the operational model as input parameters. Third, the derived requirements are embedded in the UCED optimization, which determines the least-cost dispatch and reserve scheduling while ensuring compliance with frequency security constraints.

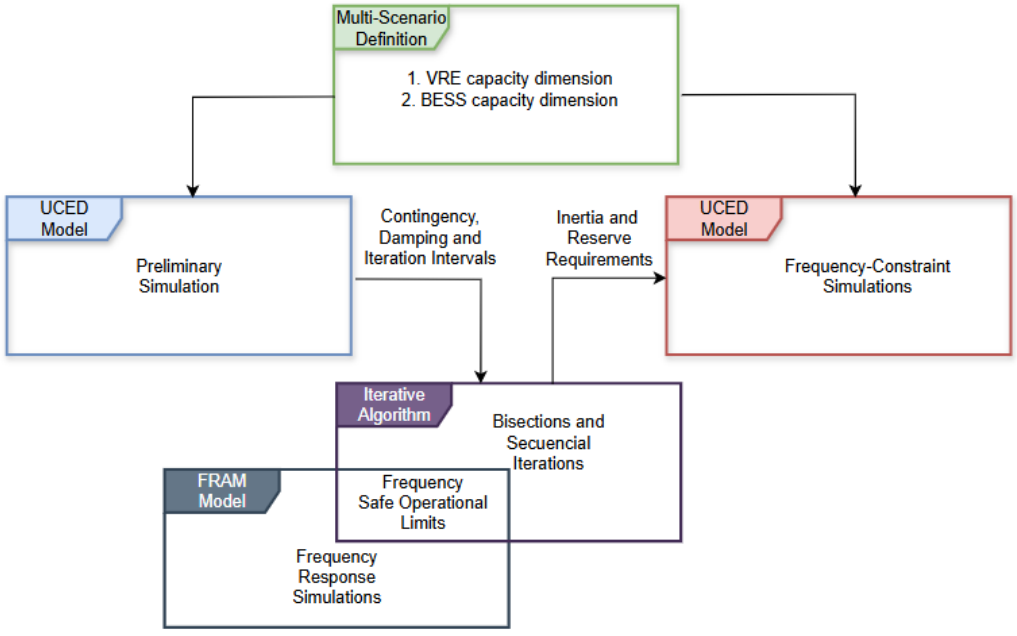

Figure 1: Workflow scheme of the UCED and FRAM link process.

This structure internalizes frequency security within the dispatch problem, ensuring that operational decisions reflect the dynamic behavior of inverter-based resources rather than treating stability as an external validation step.

2.2. Preliminary UCED Simulation for system characterization

2.2.1. Contingency Sizing

Prior to executing FRAM simulations, a preliminary UCED optimization is solved without reserve procurement constraints. This step serves to:

1. Define the contingency magnitude P_{CTG} for each time-step as the power output of the largest committed generation unit:

$$P_{\text{CTG}}(i) = \max_{u}(Power_{u,i} \cdot Committed_{u,i}) \tag{1}$$

   This ensures that contingency scenarios represent, N-1 security standard disturbances.

The output of this preliminary step comprises: (1) hourly contingency magnitudes $\Delta P_{\text{CTG}}(i)$, and (2) maximum synchronous inertia profiles $H^{\text{SIR}}_{\text{max}}(i)$. These data feed directly into the FRAM binary search algorithm, and subsequent UCED reserve scheduling.

2.2.2. Unit-level reserve capability mapping

The capability of each unit to provide frequency services is represented through (2), defined as the maximum fraction of capacity that can be allocated to each service. This parameter is computed in a preprocessing step based on technology eligibility and simplified dynamic limits.

Instead of distinguishing by service labels, the formulation groups frequency responses according to their physical behavior:

$$ReserveParticipation_{res,u} = \begin{cases} \frac{2H_u}{f_0} \cdot RoCoF_{max}, & \text{Inertia-based (VIR)} \\ \frac{1}{R_u \cdot f_0} \cdot \Delta f_{max}, & \text{Droop-based (FFR, FCR)} \\ 1, & \text{Power-limited (FFR, aFRR, mFRR)} \end{cases} \tag{2}$$

Inertia-based responses are proportional to the rate of change of frequency, droop-based responses are proportional to frequency deviation, while power-limited responses represent fast injections constrained by available capacity and ramping capabilities rather than frequency dynamics.

Table 1 summarizes the mapping between technologies, control strategies, and response types.

Table 1: Technology–service capability mapping

Technology	Control	SIR	ReserveParticipation				
			VIR	FFR	FCR	aFRR	mFRR
Hydro / Gas	Droop	Committed	–	–	Droop-based	Power-limited	Power-limited
Wind / Solar	GFL	–	–	–	Droop-based	Power-limited	Power-limited
Wind / Solar	GFM	–	Inertia-based	Droop-based	Droop-based	Power-limited	Power-limited
Battery	GFM	–	Inertia-based	Power-limited	Droop-based	Power-limited	Power-limited

Synchronous inertia is implicitly determined by unit commitment, while all reserve services are explicitly bounded through participation factors, ensuring consistency between dynamic frequency response and UCED scheduling.

2.2.3. Emergency Service Participation Matrix

Emergency frequency control actions such as Under-Frequency Load Shedding (UFLS) and Over-Frequency Demand Modulation (OFDM) are not universally or fully available across all network zones, as their deployment is typically constrained by regulatory rules, consumer categories, and system operator policies. To capture this spatial heterogeneity within the UCED framework, a participation matrix is defined to specify the maximum share of demand that can be affected by each emergency service in each zone.

Let $UFLS\_Participation_{resU,n}$ and $OFDM\_Participation_{resD,n}$ denote the participation factor of emergency type in the service *resU* or *resD* respectively, and in zone n, expressed as a fraction of the local demand. This parameter defines the upper bound of controllable load subject to emergency activation, ensuring that demand-side interventions remain physically and socially feasible.

The corresponding service limits are therefore expressed as:

2.3. Frequency Response Assessment Model (FRAM)

The FRAM is a time-domain simulation model implemented in Python that computes the system frequency trajectory following a (N-1) contingency by numerically integrating the swing equation. The model represents all frequency control layers—synchronous inertia (SIR), virtual inertia (VIR), and reserve services (FFR, FCR, aFRR, mFRR)—with their distinct activation delays and response characteristics. The FRAM's core algorithm employs sequential binary search over inertia and reserve levels to identify the minimal combination satisfying frequency stability constraints.

2.3.1. Swing Equation and System Dynamics

The dynamics of the system's center-of-inertia (COI) frequency following a power imbalance are governed by the classical swing equation, extended to include virtual inertia and multiple reserve services:

$$\frac{2 \cdot H_{\text{SIR}} \cdot S_{base}}{f_0} \frac{d\Delta f_{\text{COI}}}{dt} = P_{\text{CTG}} + P_{\text{VIR}}(t) + P_{\text{FFR}}(t) + P_{\text{FCR}}(t) + P_{\text{aFRR}}(t) + P_{\text{mFRR}}(t) + P_{\text{DMP}}(t) \tag{3}$$

2.3.2. Virtual Inertia Formulation

Virtual inertia from grid-forming IBR is implemented as a control function that injects active power proportional to the rate of change of frequency (RoCoF). Unlike synchronous inertia, which arises from rotating mass, virtual inertia is a synthetic response designed to mimic the derivative action of conventional generators. The virtual inertia power injection is formulated as:

$$P_{\text{VIR}}(t) = -\frac{2 \cdot H_{\text{VIR}} \cdot S_{base}}{f_0} \frac{d\Delta f_{\text{COI}}(t - \tau_{\text{VI}})}{dt} \tag{4}$$

This formulation is distinct from FFR in that VIR responds directly to the rate of frequency change rather than to deviation from nominal frequency. This makes virtual inertia particularly effective at limiting the initial rate of frequency decline (RoCoF) immediately after a disturbance, before deviation-based services become active.

2.3.3. Frequency Service Time-Activation Profile

The FRAM models five distinct frequency services with non-overlapping activation windows determined by control delays and delivery times. The temporal profile for each service is defined as follows

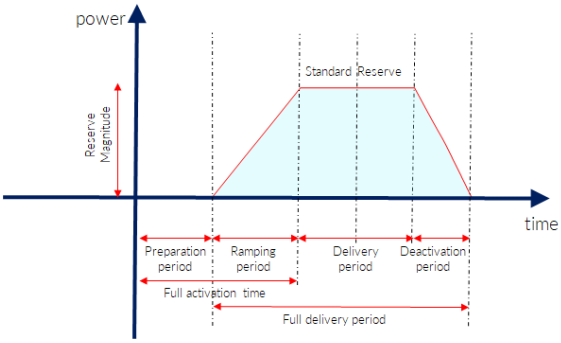

Figure 2: Generic frequency product with trapezoidal piecewise activation.

$$w^{res}(t) = \begin{cases} 0, & t < t^{res}_{\text{prep}}, \\ \dfrac{t - t^{res}_{\text{prep}}}{t^{res}_{\text{ramp}} - t^{res}_{\text{prep}}}, & t^{res}_{\text{prep}} \le t < t^{res}_{\text{ramp}}, \\ 1, & t^{res}_{\text{ramp}} \le t < t^{res}_{\text{delivery}}, \\ 1 - \dfrac{t - t^{res}_{\text{delivery}}}{t^{res}_{\text{deact}} - t^{res}_{\text{delivery}}}, & t^{res}_{\text{delivery}} \le t < t^{res}_{\text{deact}}, \\ 0, & t \ge t^{res}_{\text{deact}}. \end{cases} \tag{5}$$

2.3.4. Frequency Safe Operational Limits

The FRAM enforces three fundamental frequency stability criteria derived from grid code requirements:

$$\text{RoCoF limit:} \quad \max_t \left| \frac{df_{\text{COI}}}{dt} \right| \le \text{RoCoF}_{\text{max}} \tag{6}$$

$$\text{Nadir limit:} \quad \min_t f_{\text{COI}}(t) \ge f_{\text{min}} \tag{7}$$

$$\text{Steady-state limit:} \quad |f_{\text{COI}}(t = 60\ \text{s}) - 50| \le f_{\text{SS}} \tag{8}$$

These constraints are applied to all time steps and multiple contingency scenarios (typically defined as loss of the largest generation unit). The FRAM verifies that a candidate combination of (H_{SIR}, H_{VIR}, P_{FFR}, P_{FCR}, P_{aFRR}, P_{mFRR}) satisfies all three constraints simultaneously.

2.3.5. Binary search-based FRAM sizing with system feasibility bounds

The FRAM determines the minimum combination of inertia and reserve services required to satisfy frequency stability constraints through a sequential binary search procedure. The search space is not defined arbitrarily, but directly derived from the physical capability limits embedded in the UCED formulation through the parameter $ReserveParticipation_{res,u}$.

In particular, the maximum feasible contribution of each service is obtained by assuming that all technically eligible units operate at their full participation potential simultaneously. This implies that the upper bounds of the search space correspond to an aggregated system-wide availability rather than additional exogenous parameters.

Within this bounded space, the algorithm iteratively evaluates synchronous inertia (H_{SIR}), virtual inertia (H_{VIR}), and active power reserves (FFR, FCR, aFRR, mFRR) using a time-domain frequency simulation. For each dimension, a midpoint is tested against stability constraints (RoCoF, nadir, and steady-state deviation), and the interval is updated accordingly until convergence.

The final solution is the minimal feasible vector:

$$\mathcal{R}^* = [H^*_{\text{SIR}}, H^*_{\text{VIR}}, P^*_{\text{FFR}}, P^*_{\text{FCR}}, P^*_{\text{aFRR}}, P^*_{\text{mFRR}}], \tag{9}$$

which is subsequently passed to the UCED model as system-level requirement inputs.

2.3.6. Linking FRAM Outputs to UCED Input Parameters

The FRAM's sequential binary search produces a matrix of reserve and inertia requirements for each hourly time step and contingency scenario.
The translation of FRAM outputs into UCED parameters is performed as:

$$P_{res_U,t,c} = \text{ReserveDemand}_{res_U,n,i} \qquad \forall res_U \in \{VIRU, FFRU, FCRU, AFRRU, MFRRU\} \tag{10}$$

$$P_{res_D,t,c} = \text{ReserveDemand}_{res_D,n,i} \qquad \forall res_D \in \{FFRD, FCRD, AFRRD\} \tag{11}$$

$$H_{\text{Tot}}(t,c) = \text{InertiaDemand}_{n,i} \qquad \forall t, c \tag{12}$$

These parameters are loaded into Dispa-SET's configuration before solving the UCED model for each time step. The FRAM-derived reserve demand are translated into UCED constraints for each hour through a service-specific participation mapping. Each unit u and reserve service $res \in \{\text{VIR}, \text{FFR}, \text{FCR}, \text{aFRR}, \text{mFRR}\}$ is assigned a technical participation factor $ReserveParticipation_{u,res} \in [0,1]$, so that the committed reserve volume satisfies and meet the demand:

2.4. Unit Commitment and Economic Dispatch Model (UCED)

2.4.1. Reserve Balance Constraints in UCED

The UCED enforces reserve balance using FRAM-derived requirements. For upward and downward reserves:

$$\sum_{u,n} \text{ReserveProvision}(\text{res\_U}, u, n, i) + \text{UFLS}(\text{res\_U}, n, i) + \text{LL\_Reserve}(\text{res\_U}, n, i) = \text{ReserveDemand}(\text{res\_U}, n, i) \tag{13}$$

$$\sum_{u,n} \text{ReserveProvision}(\text{res\_D}, u, n, i) + \text{OFDM}(\text{res\_D}, n, i) + \text{LL\_Reserve}(\text{res\_D}, n, i) = \text{ReserveDemand}(\text{res\_D}, n, i) \tag{14}$$

2.4.2. Inertia Representation

Virtual inertia is included through an explicit balance constraint:

$$InertiaDemand_i \leq InertiaProvision_i + LLInertia_i \tag{15}$$

The total inertia provision is computed from committed units:

$$InertiaProvision_i = \sum_{cu} (PowerCapacity_{cu} \cdot Committed_{cu,i} \cdot InertiaConstant_{cu}) \,/\, PowerBase \tag{16}$$

2.4.3. Unit-level reserve capability constraints

The reserve capability of each unit accounts for: (i) committed units, (ii) aggregated storage units, and (iii) fast-start offline units available within the activation time.

$$\begin{aligned} ReserveProvision_{res\_U,u,i} \leq\, & PowerCapacity_{au} \cdot LoadMaximum_{u,i} \cdot ReserveParticipation_{res\_U,au,i} \\ & \cdot \Big[Committed_{u,i} + \mathbb{1}_{u \in ba} \cdot (Nunits_{au} - Committed_{u,i}) \\ & + \mathbb{1}_{StartUpTime_u \leq FullActivationTime_{res_U}} \cdot (Nunits_u - Committed_{u,i}) \Big] \end{aligned} \tag{17}$$

$$\begin{aligned} ReserveProvision_{res\_D,u,i} \leq\, & PowerCapacity_u \cdot LoadMaximum_{au,i} \cdot ReserveParticipation_{res\_D,u,i} \cdot Committed_{u,i} \\ & + \mathbb{1}_{u \in ba} \cdot StorageChargingCapacity_u \cdot (Nunits_u - Committed_{u,i}) \end{aligned} \tag{18}$$

2.4.4. Cross-service aggregated power and reserve capacity constraints

The joint provision of energy and reserves is limited by unit capacity:

$$Power_{u,i} + \sum_{res\_U} ReserveProvision_{res\_U,u,i} \leq PowerCapacity_u \cdot LoadMaximum_{u,i} \cdot Availability_{u,i} \tag{19}$$

For downward reserves:

$$Power_{u,i} - \sum_{res\_D} ReserveProvision_{res\_D,u,i} \geq PowerCapacity_u \cdot PartLoadMin_u \cdot Committed_{u,i} \tag{20}$$

2.4.5. Coupling Energy and Ancillary Service Provision

Storage operation couples energy and reserves through energy balance limits. For discharge and charge constraint as follows:

$$\begin{aligned}&Power_{u,i} \cdot TimeStep / \left(\max\left(StorageDischargeEfficiency_u, 0.0001\right)\right)\\&+ \textstyle\sum_{res\_U} ReserveProvision_{res\_U,u,i} \cdot ReserveDuration_{res\_U} / \left(\max\left(StorageDischargeEfficiency_u, 0.0001\right)\right) \leq\\&StorageInitial_u + StorageLevel_{u,i-1} + StorageInflow_{u,i} \cdot Nunits_u \cdot Time\end{aligned} \tag{21}$$

$$\begin{aligned}&StorageInput_{u,i} \cdot StorageChargingEfficiency_u \cdot TimeStep\\&+ \textstyle\sum_{res\_D} ReserveProvision_{res\_D,u,i} \cdot ReserveDuration_{res\_U} \cdot \left(max(StorageChargingEfficiency_u, 0.0001\right) \leq\\&StorageInitial_u + StorageLevel_{u,i-1} + StorageInflow_{u,i} \cdot Nunits_u \cdot Time\end{aligned} \tag{22}$$

2.4.6. Emergency frequency services constraints

Emergency actions (UFLS and OFDM) are modeled as demand-proportional limits:

$$UFLS_{res_U,n,i} \leq UFLS\_Participation_{res_U} \cdot Demand_{DA,n,i} \tag{23}$$

$$OFDM_{res_D,n,i} \leq OFDM\_Participation_{res_D} \cdot Demand_{DA,n,i} \tag{24}$$

2.4.7. Curtailed Power Constraint

Curtailed power excludes capacity allocated to reserves:

$$\begin{aligned}CurtailedPower_{n,i} = \textstyle\sum_u \big(&Nunits_u \cdot PowerCapacity_u \cdot LoadMaximum_{u,i} - Power_{u,i} + \textstyle\sum_{resU} \left(ReserveProvision_{resU,u,i}\right)\big)\\&\cdot Location_{u,n} \qquad \forall u \text{ s.t. } \textstyle\sum_{tr} Technology_{u,tr} \geq 1\end{aligned} \tag{25}$$

2.4.8. Objective Funtion

The complete UCED objective function incorporates frequency stability as a soft constraint through penalty costs:

$$\begin{aligned}SystemCost = \min \big(&\textstyle\sum_{u,i} CostFixed_u \cdot Committed_{u,i} \cdot TimeStep + \sum_{u,i} \left(CostStartUpH_{u,i} + CostShutDownH_{u,i}\right)\\&+ \textstyle\sum_{u,i} \left(CostRampUpH_{u,i} + CostRampDownH_{u,i}\right) + \sum_{u,i} CostVariable_{u,i} \cdot Power_{u,i} \cdot TimeStep\\&+ \textstyle\sum_{n,i} CostLoadShedding_{i,n} \cdot ShedLoad_{i,n} \cdot TimeStep\\&+ \textstyle\sum_{i,n} VOLL_{Power} \cdot LLPower_{i,n} \cdot TimeStep + \sum_{u,i} VOLL_{Ramp} \cdot LLRamp_{u,i} \cdot TimeStep\\&+ \textstyle\sum_{res,n} VOLL_{Reserve} \cdot LLReserve_{res,i,n} \cdot TimeStep + \sum_{res,n} VOLL_{Inertia} \cdot LLInertia_{res,i,n} \cdot TimeStep\\&+ \textstyle\sum_{res,n} CostUFLS_{i,n} \cdot UFLS_{res,n,i} \cdot TimeStep + \sum_{res,n} CostOFDM_{i,n} \cdot OFDM_{res,n,i} \cdot TimeStep\\&+ \textstyle\sum_{s,i} CostOfSpillage \cdot Spillage_{s,i} \cdot TimeStep + \sum_s WaterValue \cdot WaterSlack_s\big)\end{aligned} \tag{26}$$

The objective function minimizes total system cost while enforcing security through penalty terms. A hierarchy of penalties ensures the following priority: (i) energy balance, (ii) reserve provision, (iii) emergency actions (UFLS/OFDM), and (iv) involuntary load shedding. High penalty values (VoLL) ensure that violations occur only when strictly necessary.

2.4.9. Post-Processing Metrics: VRE Curtailment, Reserve Allocation, and Penetration

To quantify the operational effects of inverter-based resources (IBRs) under high renewable penetration, three rates are evaluated: VRE curtailment, VRE reserve allocation, and VRE penetration. All metrics are computed over VRE units and time-step periods.

VRE Curtailment Rate. Share of available VRE energy that is curtailed:

$$CurtailmentRate = \textstyle\sum_{\mathrm{i}} \mathrm{CurtailedPower_i} \quad / \quad \left(\sum_{\mathrm{u,i}} \mathrm{Power_{u,i}} + \sum_{\mathrm{i}} \mathrm{CurtailedPower_i}\right) \cdot 100, \quad \nVdash_{u \in tr} \tag{27}$$

VRE Reserve Allocation Rate. Fraction of VRE capacity committed to reserve services (e.g., VIR, FFR):

$$ReserveAllocationRate = \textstyle\sum_{\mathrm{u,i}} \mathrm{ReserveProvision_{u,i}} \quad / \quad \left(\sum_{\mathrm{u,i}} \mathrm{Power_{u,i}} + \sum_{\mathrm{i}} \mathrm{CurtailedPower_i}\right) \cdot 100, \quad \nVdash_{u \in tr} \tag{28}$$

VRE Penetration Rate. Contribution of VRE generation to total system demand:

$$PenetrationRate = \textstyle\sum_{\mathrm{u,i}} \mathrm{Power_{u,i}} \quad / \quad \left(\sum_{\mathrm{u,i}} \mathrm{Power_{u,i}} + \sum_{\mathrm{i}} \mathrm{CurtailedPower_i}\right) \cdot 100, \quad \nVdash_{u \in tr} \tag{29}$$

These rates enable a consistent comparison between scenarios where IBRs operate solely as energy suppliers and scenarios where they also provide frequency-support reserves. This distinction reveals whether frequency-security constraints limit renewable integration or whether IBR-based reserve capabilities enhance system flexibility and VRE utilization.

3. CASE STUDY AND SCENARIO DEFINITION

Bolivia is selected as case study due to its combination of high renewable-resource potential and weak regional interconnection characteristics, which make frequency security and operational flexibility particularly relevant under high shares of inverter-based resources (IBRs). The country exhibits excellent solar conditions in the Altiplano region together with significant wind potential in the southern and eastern areas, supporting large-scale deployment of wind and solar generation. At the same time, despite its central geographic location in South America, Bolivia remains weakly interconnected with neighboring systems, and regional integration projects are expected to evolve only gradually in the coming decades. As a result, the Bolivian National Interconnected System (SIN) provides a suitable benchmark for studying low-inertia operation under isolated or weakly interconnected conditions.

The objective of this study is not to reproduce a realistic expansion pathway for the Bolivian system, but rather to evaluate how increasing penetration of IBRs modifies unit commitment, reserve allocation, and frequency-security requirements. For this purpose, a structured multi-dimensional scenario framework is developed combining: (i) progressive VRE penetration levels, (ii) different reserve configurations, and (iii) incremental BESS deployment. This approach enables a sensitivity analysis of techno-economic and operational indicators associated with future low-inertia systems, including flexibility requirements, reserve utilization, renewable integration capability, and frequency-security performance.

3.1. Bolivian Power System Description and Configuration

The study considers a 2030 representation of the Bolivian SIN aggregated into four operational zones (NO, OR, CE, and SU), including thermal, hydro, wind, solar, and BESS technologies together with inter-zonal transmission constraints. The Bolivian system is characterized by moderate industrialization and a predominantly residential demand structure, resulting in relatively pronounced daily demand variations and strong dependence on operational flexibility from conventional generation.

The UCED model is parameterized using installed generation capacities, technology-specific operational constraints, zonal demand profiles, and inter-zonal transfer capacities. In parallel, the FRAM framework incorporates system-wide frequency-security limits and reserve activation dynamics for VIR, FFR, FCR, aFRR, and mFRR services. Table 2 summarizes the main assumptions adopted in the case study.

Table 2: Bolivian SIN 2030 case-study configuration

Generation Mix		**Thermal**	**Hydro**	**BESS**	**Solar**	**Wind**	**Total**
Installed Capacity [MW]		2449	1221	1200	475	392	5737
Share of Capacity [%]		42.7	21.3	20.9	8.3	6.8	100
Technology		GTUR/STUR	HDAM/HROR	BATS	PHOT	WTON	–
Efficiency		0.35	0.80	1.00	1.00	1.00	–
Ramp Rate [p.u./min]		0.0067	0.0067	1.00	0.02	0.02	–
Minimum Output [%]		40–60	30	0	0	0	–
Inertia Constant [s]		3.3–4.2	3.7	0	0	0	–
Fuel Cost [USD/MWh]		16–25	0	0	0	0	–
Demand and Network Configuration							
Zone	NO	OR	CE	SU			
Average Demand [MW]	352	598	327	306			
Peak Demand [MW]	523	1097	480	396			
Minimum Demand [MW]	201	266	180	186			
Interconnection	NO→CE	OR→CE	CE→SU	NO→OR			
NTC [MW]	442	1023	445	140			
Frequency-Security Parameters							
Rated Frequency [Hz]	50	RoCoF Limit [Hz/s]	-0.5	Frequency Nadir [Hz]	49.2	Recovery Time [s]	60
Reserve Activation Parameters							
Service	VIR	FFR	FCR	aFRR	mFRR		
Prep Delay [s]	0.1	1	4	30	480		
Ramp Time [s]	0.15	2	10	270	420		
Delivery Time [s]	1.5	60	180	480	–		
Deactivation Time [s]	6	300	300	901	–		

3.2. Multi-Dimensional Scenario Framework

A multi-dimensional scenario framework is developed to evaluate the operational role of inverter-based resources (IBRs) in unit commitment and optimal dispatch under increasing renewable penetration levels. In this study, IBRs are represented by utility-scale wind and solar generation together with BESS-based frequency-support services, enabling the assessment of both renewable integration and inverter-driven system flexibility. The proposed scenarios do not represent a realistic expansion pathway for the Bolivian power system. Instead, they are designed as a structured sensitivity analysis to investigate how increasing shares of IBRs affect dispatch behavior, reserve allocation, flexibility requirements, and frequency-security performance in low-inertia systems. The framework combines three dimensions: (i) VRE penetration, (ii) reserve configuration, and (iii) BESS deployment. Six VRE scenarios (V1–V6) are defined through progressive increases in installed wind and solar capacity. Three reserve configurations are considered. Scenario R0 represents unconstrained operation without explicit reserve or frequency-security constraints, allowing the model to determine the naturally available flexibility from the economic dispatch. Scenario R1 incorporates conventional frequency services through SIR, FCR, aFRR, and mFRR. Scenario R2 extends R1 by enabling advanced inverter-based services through VIR and FFR. To evaluate the contribution of storage-supported IBR flexibility, seven BESS deploy-

ment levels are analyzed. Scenario B0 assumes no installed BESS capacity and therefore no participation of advanced inverter-based reserves. Scenarios B1–B6 progressively increase BESS capacity, enabling larger contributions of VIR and FFR from inverter-based technologies.

Table 3: Multi-dimensional scenario framework

VRE Configuration		**V1**	**V2**	**V3**	**V4**	**V5**	**V6**
Installed Capacity	Solar [MW]	475	950	1425	1900	2375	2850
	Wind [MW]	392	784	1176	1568	1960	2352
	Total VRE [MW]	867	1734	2601	3468	4335	5202
Reserves Configuration							
R0	No reserve or frequency-security constraints						
R1	SIR + FCR + aFRR + mFRR						
R2	SIR + VIR + FFR + FCR + aFRR + mFRR						
BESS Configuration		**B0**	**B1**	**B2**	**B3**	**B4**	**B5**	**B6**
BESS Capacity	Power [MW]	0	800	1600	2400	3200	4000	4800
	Energy [MWh]	0	6400	12800	19200	25600	32000	38400

The proposed framework enables the analysis of how storage-supported IBR services modify system operation under high renewable penetration scenarios. In particular, it allows the evaluation of techno-economic indicators associated with future low-inertia systems, including reserve utilization, operational flexibility, renewable integration capability, and frequency-security performance.

The proposed framework enables the analysis of how storage-supported IBR services modify system operation under high renewable penetration scenarios. In particular, it allows the evaluation of techno-economic indicators associated with future low-inertia systems, including reserve utilization, operational flexibility, renewable integration capability, and frequency-security performance.

4. RESULTS

This section evaluates the impact of frequency-security constraints and inverter-based frequency services on the operation of the Bolivian SIN under increasing renewable penetration scenarios. The analysis is divided into four parts: (i) dynamic frequency assessment using the proposed FRAM framework, (ii) reserve sizing requirements across scenarios, (iii) UCED dispatch impacts, and (iv) techno-economic implications of frequency-constrained operation.

4.1. Frequency Stability Assessment (FRAM Outputs)

4.1.1. Frequency Response and Reserve Sizing with set R1 services

Table 4 presents the results of the power swing equation, incorporating different values of FCR. The results indicate that the minimum RoCoF threshold of 0.5 Hz/s is met, as FCR is proportionally responding to the frequency deviation. This allows frequency recovery before reaching critical levels below 49.2 Hz without the subsequent activation of additional reserves.

Table 4: Power swing equation results with the incorporation of fast frequency reserves.

Contingency	Contingency [MW]	System Inertia [s]	FCR [MW]	aFRR [MW]	mFRR [MW]	Min Frequency [Hz]	Min RoCoF [Hz/s]	Frequency Nadir [Hz]	RoCoF [Hz/s]	State
1	194	10	121	194	194	49.20	-0.5	45.84	-0.48	Unstable
2	194	10	135	194	194			46.52	-0.48	Unstable
3	194	10	161	194	194			47.22	-0.48	Unstable
4	194	10	218	194	194			48.23	-0.48	Unstable
5	194	10	237	194	194			49.21	-0.40	Stable

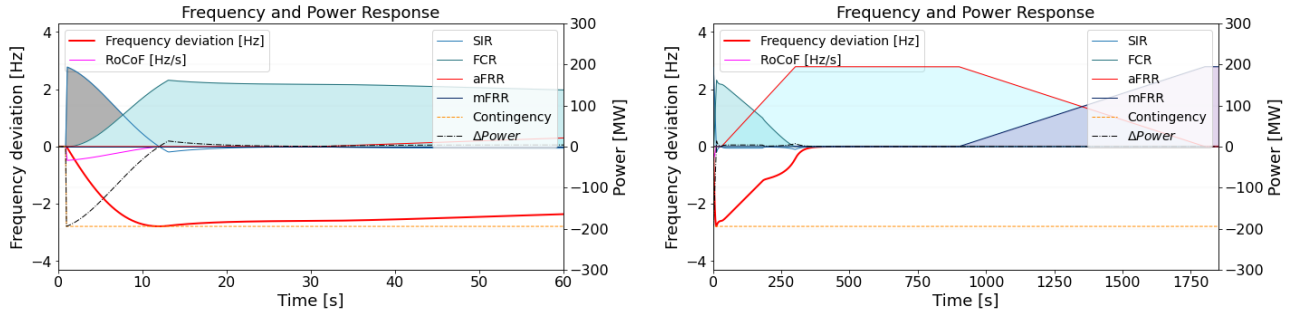

(a) Frequency and Power Excursion first 60 seconds

(b) Frequency and Power Excursion full response

Figure 3: Frequency and Power Excursions for Contingency 3

Table 5 summarizes key system capacity metrics and the range of expected contingency sizes obtained from the preliminary UCED simulation of the Bolivian SIN. These results define feasible operating ranges of system capabilities and are used to establish the bounds for the binary search of reserve requirements in the FRAM frequency response analysis.

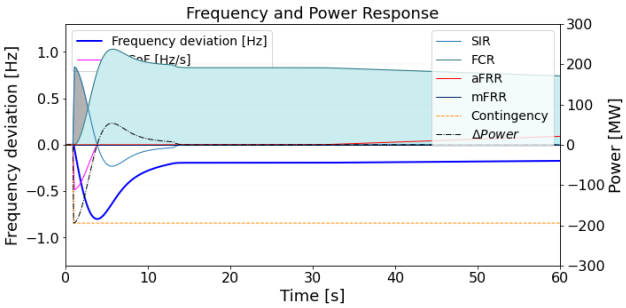

(a) Frequency and Power Excursion first 60 seconds

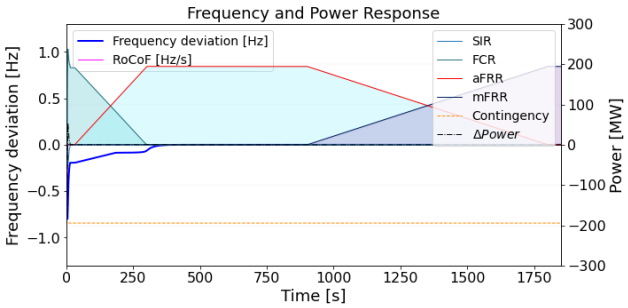

(b) Frequency and Power Excursion full response

Figure 4: Frequency and Power Excursions for Contingency 5

Table 5: Contingency and Reserves Iteration Ranges for FRAM (No IBR)

Parameter	Non-Frequency-Constrained Scenarios (No IBR)						Frequency-Constrained Scenarios (No IBR)					
	V1-R0-B0	V2-R0-B0	V3-R0-B0	V4-R0-B0	V5-R0-B0	V6-R0-B0	V1-R1-B0	V2-R1-B0	V3-R1-B0	V4-R1-B0	V5-R1-B0	V6-R1-B0
Contingency Min (MW)	63.54	46.46	48.81	47.05	46.37	35.09	40.90	39.88	46.24	39.16	36.00	36.00
Contingency Avg (MW)	136.64	134.70	134.72	145.78	150.06	155.87	106.61	110.07	108.92	105.59	107.05	106.46
Contingency Max (MW)	194.63	194.63	194.63	194.63	194.63	194.63	194.63	194.63	194.63	194.63	194.63	194.63
Inertia Capacity Min (s)	0.00	0.00	0.00	0.00	0.00	0.00	0.00	0.00	0.00	0.00	0.00	0.00
Inertia Capacity Max (s)	14.69	14.69	14.69	14.69	14.69	14.69	14.69	14.69	14.69	14.69	14.69	14.69
FCR Capacity Min (MW)	0.00	0.00	0.00	0.00	0.00	0.00	0.00	0.00	0.00	0.00	0.00	0.00
FCR Capacity Max (MW)	0.00	0.00	0.00	0.00	0.00	0.00	1451.89	1729.21	2006.53	2283.86	2561.18	2838.49

Table 6 summarizes the reserve-provision for the V1–V6 scenarios of the 2030 Bolivian system. The results show that reserve sizing does not necessarily increase with VRE penetration, but depends primarily on the adopted *N*-1 contingency criterion, the inertial characteristics of the system, and the time-dependent availability of frequency-support services across the system.

Table 6: Frequency Reserves Provision and Emergency Services Across Scenarios (No IBR)

Parameter	Non-Frequency-Constrained Scenarios (No IBR)						Frequency-Constrained Scenarios (No IBR)					
	V1-R0-B0	V2-R0-B0	V3-R0-B0	V4-R0-B0	V5-R0-B0	V6-R0-B0	V1-R1-B0	V2-R1-B0	V3-R1-B0	V4-R1-B0	V5-R1-B0	V6-R1-B0
Avg. Inertia (GW·s)	6.87	5.57	4.40	3.93	3.68	3.54	12.36	10.38	9.77	10.18	10.55	11.08
Avg. FCRU (MW)	0.00	0.00	0.00	0.00	0.00	0.00	156.75	154.30	154.36	168.58	174.14	181.62
Avg. FCRD (MW)	0.00	0.00	0.00	0.00	0.00	0.00	156.52	154.16	154.23	168.48	174.04	181.53
Avg. aFRRU (MW)	0.00	0.00	0.00	0.00	0.00	0.00	136.61	134.68	134.69	145.76	150.04	155.85
Avg. aFRRD (MW)	0.00	0.00	0.00	0.00	0.00	0.00	136.61	134.67	134.67	145.76	150.03	155.84
Avg. mFRRU (MW)	0.00	0.00	0.00	0.00	0.00	0.00	136.61	134.68	134.69	145.76	150.04	155.85
Cum. UFLS (MW)	0.00	0.00	0.00	0.00	0.00	0.00	0.00	0.00	0.00	0.00	0.00	0.00
Cum. OFDM (MW)	0.00	0.00	0.00	0.00	0.00	0.00	2004.69	1288.23	1315.12	863.84	969.67	955.37

4.1.2. Frequency Response and Reserve sizing with set R2 services

The progression from Scenario 1 (inertia-only) to Scenario 5 (with VIR and FFR upgrade and additional reserves) demonstrates that frequency stability emerges from the coordinated action of multiple services. FCR alone cannot rescue an unstable scenario; the combination of VIR, FFR is required for compliance. This reinforces the need for multi-service coordination in grid code requirements.

Table 7: Power swing equation results with the incorporation of fast frequency reserves.

Contingency	Contingency [MW]	Synchronous Inertia Constant [s]	Virtual Inertia Constant [s]	SIR [MW]	VIR [MW]	FFR [MW]	FCR [MW]	aFRR [MW]	mFRR [MW] [Hz]	Min Frequency [Hz/s]	Min RoCoF [Hz]	Frequency Nadir [Hz/s]	RoCoF	State
6	194	8.50	1.50	164.73	29.07	169.68	165.32	194	194	49.20	-0.50	48.31	-0.48	Unstable
7	194	6.50	2.25	143.88	49.80	175.79	165.62	194	194			48.30	-0.55	Unstable
8	194	3.75	4.50	88.01	105.61	178.69	165.72	194	194			48.30	-0.59	Unstable
9	194	3.75	7.75	63.22	130.66	322.49	181.44	194	194			49.22	-0.42	Stable
10	194	1.50	12	21.55	172.44	282.00	181.39	194	194			49.22	-0.36	Stable

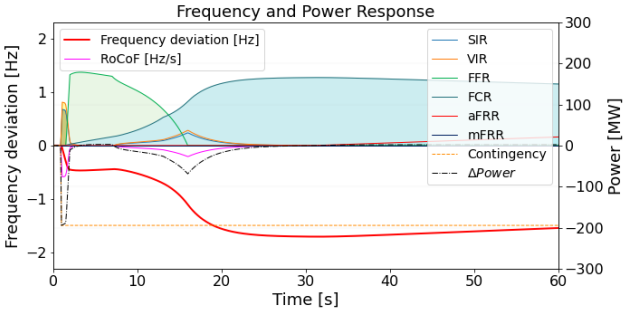

(a) Frequency and Power Excursion first 30 seconds

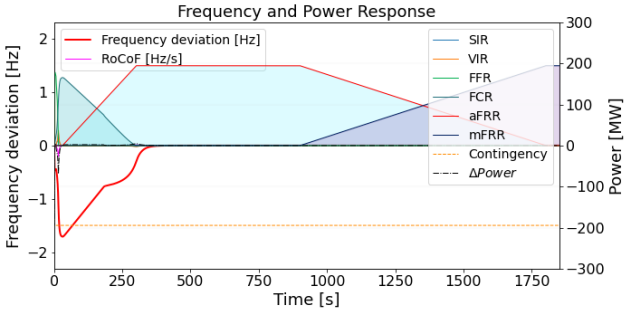

(b) Frequency and Power Excursion full response

Figure 5: Frequency and Power Excursion for Contingency 8

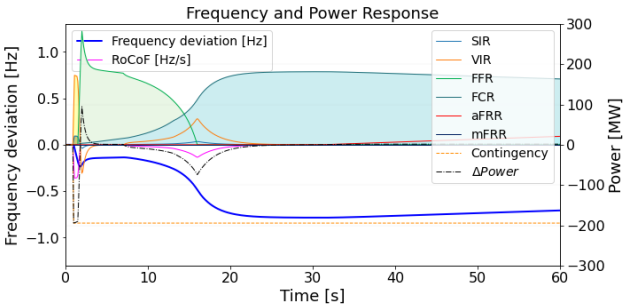

(a) Frequency and Power Excursion first 30 seconds

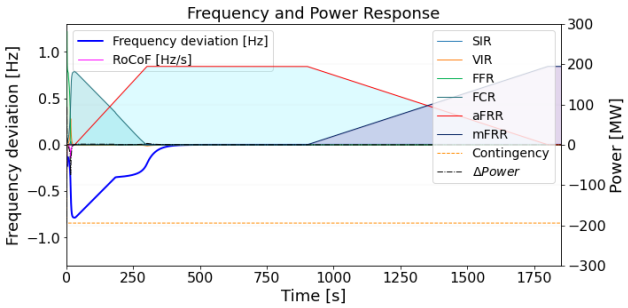

(b) Frequency and Power Excursion full response

Figure 6: Comparison of Frequency and Power Excursion for Contingency 10

Table 8: Contingency and Reserves Iteration Ranges for FRAM (with IBR)

Parameter	R0 Scenarios						R2 Scenarios					
	V1-R0-B1	V2-R0-B2	V3-R0-B3	V4-R0-B4	V5-R0-B5	V6-R0-B6	V1-R2-B1	V2-R2-B2	V3-R2-B3	V4-R2-B4	V5-R2-B5	V6-R2-B6
Contingency Min (MW)	68.87	51.91	42.91	57.33	63.02	55.00	46.24	46.66	42.91	52.39	63.86	43.78
Contingency Avg (MW)	142.17	137.52	137.62	141.59	148.52	155.51	114.00	132.97	135.55	139.48	146.91	153.92
Contingency Max (MW)	194.63	194.63	194.63	194.63	194.63	194.63	194.63	194.63	194.63	194.63	194.63	194.63
Inertia Capacity Min (GW·s)	0.00	0.00	0.00	0.00	0.00	0.00	0.00	0.00	0.00	0.00	0.00	0.00
Inertia Capacity Max (GW·s)	14.69	14.69	14.69	14.69	14.69	14.69	14.69	14.69	14.69	14.69	14.69	14.69
Virtual Inertia Capacity Min (GW·s)	0.00	0.00	0.00	0.00	0.00	0.00	0.00	0.00	0.00	0.00	0.00	0.00
Virtual Inertia Capacity Max (GW·s)	0.00	0.00	0.00	0.00	0.00	0.00	224	448	672	896	1120	1344
FFR Capacity Min (MW)	0.00	0.00	0.00	0.00	0.00	0.00	0.00	0.00	0.00	0.00	0.00	0.00
FFR Capacity Max (MW)	0.00	0.00	0.00	0.00	0.00	0.00	640	1280	1920	2560	3200	3840
FCR Capacity Min (MW)	0.00	0.00	0.00	0.00	0.00	0.00	0.00	0.00	0.00	0.00	0.00	0.00
FCR Capacity Max (MW)	0.00	0.00	0.00	0.00	0.00	0.00	2091.89	3009.53	3926.53	4843.86	5761.18	6678.49

Table 9: Frequency Reserves Provision and Emergency Services Across Scenarios (with IBR)

Parameter	Non-Frequency-Constrained Scenarios (with IBR)						Frequency-Constrained Scenarios (with IBR)					
	V1-R0-B1	V2-R0-B2	V3-R0-B3	V4-R0-B4	V5-R0-B5	V6-R0-B6	V1-R2-B1	V2-R2-B2	V3-R2-B3	V4-R2-B4	V5-R2-B5	V6-R2-B6
Avg. Inertia (GW·s)	6.71	5.65	4.33	3.73	3.62	3.60	12.27	5.80	4.40	3.84	3.77	3.71
Avg. VIR (MW)	0.00	0.00	0.00	0.00	0.00	0.00	89.59	102.59	101.64	106.48	113.52	121.44
Avg. FFRU (MW)	0.00	0.00	0.00	0.00	0.00	0.00	154.55	230.39	236.63	240.90	253.30	262.27
Avg. FFRD (MW)	0.00	0.00	0.00	0.00	0.00	0.00	154.15	229.87	236.42	240.85	253.30	262.27
Avg. FCRU (MW)	0.00	0.00	0.00	0.00	0.00	0.00	123.52	119.51	119.74	123.49	130.44	137.47
Avg. FCRD (MW)	0.00	0.00	0.00	0.00	0.00	0.00	123.52	119.51	119.74	123.49	130.44	137.47
Avg. aFRRU (MW)	0.00	0.00	0.00	0.00	0.00	0.00	142.15	137.51	137.60	141.57	148.50	155.49
Avg. aFRRD (MW)	0.00	0.00	0.00	0.00	0.00	0.00	142.15	137.51	137.59	141.57	148.50	155.49
Avg. mFRRU (MW)	0.00	0.00	0.00	0.00	0.00	0.00	142.15	137.51	137.60	141.57	148.50	155.49
Cum. UFLS (MW)	0.00	0.00	0.00	0.00	0.00	0.00	147.19	0.00	0.00	0.00	0.00	0.00
Cum. OFDM (MW)	0.00	0.00	0.00	0.00	0.00	0.00	3676.92	4566.9	1880.14	386.77	42.72	5.71

4.2. Dispatch Comparison (UCED Results)

Tables 10 and 11 reveal that frequency constraints (R1) effectively anchor thermal generation in the dispatch, limiting its displacement even at high VRE levels, while hydro output is partially redirected toward reserve provision. This reallocation constrains VRE integration, leading to increasing curtailment. With IBR-based services (R2), these constraints ease, allowing thermal reduction and near-complete recovery of renewable generation.

Table 10: Dispatch comparison between scenarios (No IBR)

Technology	Unit	Non-Frequency-Constrained Scenarios (No IBR)						Frequency-Constrained Scenarios (No IBR)					
		V1-R0-B0	V2-R0-B0	V3-R0-B0	V4-R0-B0	V5-R0-B0	V6-R0-B0	V1-R1-B0	V2-R1-B0	V3-R1-B0	V4-R1-B0	V5-R1-B0	V6-R1-B0
Hydro	[TWh]	5.11	5.19	5.45	5.99	6.03	6.10	4.73	4.92	5.13	5.20	5.08	5.07
Thermal	[TWh]	5.34	3.09	1.49	0.56	0.30	0.24	6.33	4.43	3.39	3.32	3.53	3.83
Wind	[TWh]	1.44	2.87	4.13	5.16	5.92	6.16	1.23	2.36	3.20	3.50	3.46	3.38
Solar	[TWh]	1.09	2.16	2.96	3.45	3.41	3.34	0.93	1.81	2.43	2.51	2.58	2.38
Biomass	[TWh]	0.91	0.77	0.51	0.27	0.17	0.14	0.69	0.56	0.30	0.10	0.08	0.07
Curtailment	[TWh]	0.00	0.02	0.48	1.49	3.29	5.65	0.37	0.88	1.94	4.08	6.58	9.39

Table 11: Dispatch comparison between scenarios (with IBR)

Technology	Unit	Non-Frequency-Constrained Scenarios (with IBR)						Frequency-Constrained Scenarios (with IBR)					
		V1-R0-B1	V2-R0-B2	V3-R0-B3	V4-R0-B4	V5-R0-B5	V6-R0-B6	V1-R2-B1	V2-R2-B2	V3-R2-B3	V4-R2-B4	V5-R2-B5	V6-R2-B6
Hydro	[TWh]	5.13	5.19	5.27	5.55	5.76	5.80	5.06	5.19	5.27	5.52	5.71	5.73
Thermal	[TWh]	5.34	3.08	1.34	0.36	0.07	0.02	6.29	3.08	1.34	0.37	0.07	0.03
Wind	[TWh]	1.44	2.88	4.31	5.75	7.19	8.62	1.44	2.88	4.31	5.75	7.19	8.60
Solar	[TWh]	1.09	2.17	3.26	4.35	5.44	6.52	1.09	2.17	3.26	4.35	5.44	6.52
Biomass	[TWh]	0.92	0.78	0.53	0.25	0.04	0.01	0.69	0.77	0.53	0.26	0.05	0.02
Batteries	[TWh]	0.60	1.65	2.57	3.79	4.24	4.45	0.91	2.49	3.70	5.21	7.25	7.85
Curtailment	[TWh]	0.00	0.00	0.00	0.00	0.00	0.01	0.00	0.00	0.00	0.00	0.00	0.03

4.3. Operational and Economic Impact (UCED Results)

The UCED results show pronounced divergences once frequency constraints are enforced. In the absence of IBR services (R1), system cost rises and VRE penetration is more limited, accompanied by higher emissions and curtailment levels reaching nearly 62%. When IBR-based services are enabled (R2), these metrics collapse: costs and emissions in V6 are reduced by more than 98–99%, and curtailment becomes negligible ($<$0.3%). While this shift reflects the substitution of synchronous reserves by fast-response services, the

magnitude of the change is also influenced by the scale of BESS deployment, which contributes substantial energy-shifting capability. Therefore, the observed gains combine improved frequency-service provision with the effect of large-scale storage, rather than being attributable to reserve modeling alone.

Table 12: Techno-Economic and Environmental Comparison (No IBR)

Parameter	Non-Frequency-Constrained Scenarios (No IBR)						Frequency-Constrained Scenarios (No IBR)					
	V1-R0-B0	V2-R0-B0	V3-R0-B0	V4-R0-B0	V5-R0-B0	V6-R0-B0	V1-R1-B0	V2-R1-B0	V3-R1-B0	V4-R1-B0	V5-R1-B0	V6-R1-B0
Total System Cost [Meur]	222.09	137.77	71.41	29.52	16.90	13.60	253.32	185.89	139.41	131.18	144.41	153.07
Avg. Spillage [MW]	81.02	87.67	93.51	94.25	94.97	96.76	136.52	126.76	129.58	129.22	129.07	129.34
Avg. Emissions [kg$CO_{2,eq}$/MWh]	349.90	202.61	97.87	36.72	19.65	15.70	415.02	290.45	222.23	217.52	231.56	250.90
Avg. Shadow Price [eur/MWh]	45.45	43.73	35.41	25.14	20.88	12.01	24.62	21.99	11.72	1.98	0.84	0.23
VRE Penetration [%]	100	99.56	93.65	85.25	73.97	62.71	85.22	82.59	74.34	59.56	47.88	38.03
VRE Curtailment [%]	0.00	0.44	6.35	14.75	26.06	37.29	14.78	17.41	25.66	40.44	52.12	61.97
VRE Curtailment for Reserves [%]	0.00	0.00	0.00	0.00	0.00	0.00	8.84	4.61	3.06	2.62	2.00	1.95

Table 13: Techno-Economic and Environmental Comparison (with IBR)

Parameter	Non-Frequency-Constrained Scenarios (with IBR)						Frequency-Constrained Scenarios (with IBR)					
	V1-R0-B0	V2-R0-B0	V3-R0-B0	V4-R0-B0	V5-R0-B0	V6-R0-B0	V1-R1-B0	V2-R1-B0	V3-R1-B0	V4-R1-B0	V5-R1-B0	V6-R1-B0
Total System Cost [Meur]	221.12	135.55	65.38	21.07	3.91	1.26	252.09	136.97	66.53	22.02	4.14	1.81
Avg. Spillage [MW]	80.63	90.02	143.50	269.23	476.43	749.97	163.96	89.84	144.94	273.64	486.73	747.15
Avg. Emissions [kg$CO_{2,eq}$/MWh]	349.91	201.49	87.49	23.33	4.35	1.22	412.37	201.72	88.05	24.33	4.56	1.92
Avg. Shadow Price [eur/MWh]	41.05	41.38	29.21	20.37	2.56	0.63	26.11	31.01	32.56	12.35	3.60	0.89
VRE Penetration [%]	100.00	100.00	100.00	99.99	99.98	99.95	99.95	100.00	99.99	99.98	99.99	99.78
VRE Curtailment [%]	0.00	0.00	0.00	0.01	0.02	0.05	0.05	0.00	0.01	0.02	0.01	0.22
VRE Curtailment for Reserves [%]	0.00	0.00	0.00	0.00	0.00	0.00	0.00	0.00	0.00	0.00	0.00	0.00

4.4. System Reserve Adequacy (UCED Multi-Scenario Analysis)

From a system adequacy perspective, the constraint shifts from energy balance to fast-response capability. Under (R1), thermal units dominate FCR and aFRR provision, requiring sustained commitment and leading to both higher curtailment and system costs. In (R2), BESS provide most VIR and FFR, reducing the need for synchronous support; however, at the assumed capacities, they also absorb surplus generation.

Table 14: Technology Contribution to Reserve Provision Across Scenarios

Reserve	Technology	Frequency-Constrained Scenarios (No IBR)						Frequency-Constrained Scenarios(with IBR)					
		V1-R1-B0	V2-R1-B0	V3-R1-B0	V4-R1-B0	V5-R1-B0	V6-R1-B0	V1-R2-B1	V2-R2-B2	V3-R2-B3	V4-R2-B4	V5-R2-B5	V6-R2-B6
VIR	Batteries [%]	0.00	0.00	0.00	0.00	0.00	0.00	100.00	100.00	100.00	100.00	100.00	100.00
FFR	Batteries [%]	0.00	0.00	0.00	0.00	0.00	0.00	100.00	100.00	100.00	100.00	100.00	100.00
FCR	Hydro [%]	29.58	27.46	24.51	22.95	23.20	23.63	25.84	18.33	17.39	13.50	10.78	10.75
	Thermal [%]	62.20	62.74	64.28	64.36	63.71	62.05	59.42	72.84	75.93	79.08	81.19	81.25
	Wind [%]	3.94	4.25	5.11	5.58	5.80	6.74	0.00	0.00	0.00	0.00	0.00	0.00
	Solar PV [%]	2.68	3.21	3.18	3.10	2.92	3.00	0.00	0.00	0.00	0.00	0.00	0.00
	Bio [%]	1.60	2.34	2.92	4.02	4.36	6.74	1.85	0.71	1.50	1.98	2.70	2.80
	Batteries [%]	0.00	0.00	0.00	0.00	0.00	0.00	12.89	8.13	5.18	5.43	5.33	5.20
aFRR	Hydro [%]	30.06	24.16	22.14	23.65	25.45	27.80	19.73	5.81	5.86	3.86	2.63	2.36
	Thermal [%]	54.99	61.23	61.97	58.15	54.60	49.26	60.86	93.90	93.80	95.70	96.93	97.17
	Wind [%]	4.36	3.45	3.02	3.02	2.70	2.91	3.65	0.00	0.00	0.00	0.00	0.00
	Solar PV [%]	2.21	2.58	2.47	2.60	1.90	2.19	5.51	0.00	0.00	0.00	0.00	0.00
	Bio [%]	8.39	8.51	10.39	12.58	15.35	17.85	11.24	0.09	0.16	0.25	0.31	0.33
	Batteries [%]	0.00	0.00	0.00	0.00	0.00	0.00	8.18	0.20	0.18	0.19	0.14	0.13
mFRR	Hydro [%]	30.19	23.77	21.73	23.43	25.64	27.72	20.72	5.85	5.91	3.90	2.63	2.32
	Thermal [%]	57.75	62.29	63.11	58.69	54.19	48.92	60.52	93.85	93.74	95.66	96.93	97.22
	Wind [%]	3.05	3.40	3.08	3.21	2.83	3.12	3.65	0.00	0.00	0.00	0.00	0.00
	Solar PV [%]	1.43	1.77	1.57	1.82	1.68	2.10	5.51	0.00	0.00	0.00	0.00	0.00
	Bio [%]	7.58	8.77	10.51	12.78	15.66	18.15	10.35	0.09	0.17	0.25	0.30	0.33
	Batteries [%]	0.00	0.00	0.00	0.00	0.00	0.00	8.40	0.21	0.18	0.19	0.14	0.13

5. CONCLUSIONS

This paper proposes a coupled FRAM–UCED framework to incorporate frequency-security requirements into operational planning and to assess the role of IBRs in low-inertia systems. The results show that frequency constraints directly influence system operation, shaping the generation mix, cost structure, and renewable integration. In the absence of inverter-based services (R1), frequency security is maintained through increased commitment of synchronous generation, leading to higher operating costs, increased CO_2 emissions, and reduced renewable integration. These effects are reflected in higher marginal prices at low renewable penetration and increasing curtailment as penetration grows. When IBR-based services are enabled (R2), VIR and FFR reduce the reliance on synchronous inertia, enabling lower thermal commitment. This results in improved renewable integration, lower costs and emissions, and a reconfiguration of the reserve portfolio toward fast-response technologies, primarily BESS, while conventional units continue to provide slower services such as aFRR and mFRR. The results also reflect the combined contribution of storage-driven energy shifting and frequency-service provision. By capturing these effects within a unified formulation, the proposed framework provides a consistent basis to analyze their interaction, while highlighting the sensitivity of system outcomes to storage capacity and operational assumptions. A key aspect of the formulation is the explicit representation of frequency services over their activation period, accounting jointly for power and energy requirements. This enables a more consistent characterization of frequency support compared to headroom-based approaches and provides a clearer assessment of the operational value of IBR-based services. Dynamic requirements are derived using a system-level frequency representation based on an equivalent inertia formulation. While this

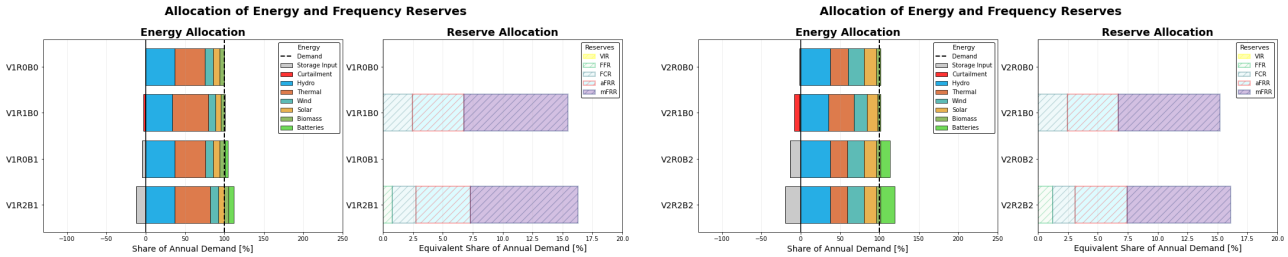

(a) Scenario 1

(b) Scenario 2

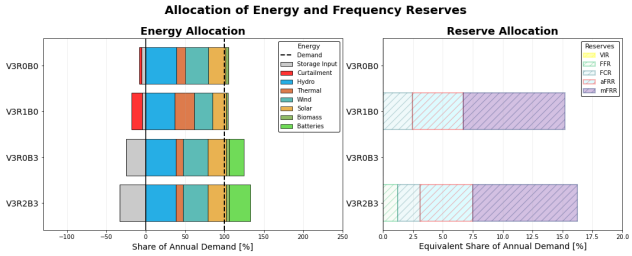

(c) Scenario 3

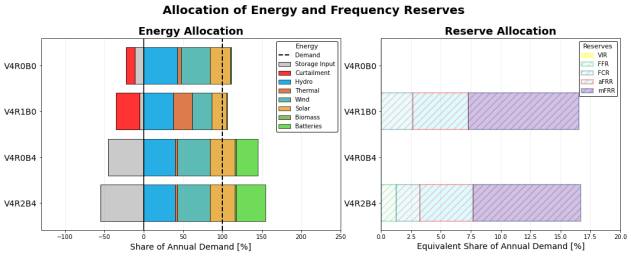

(d) Scenario 4

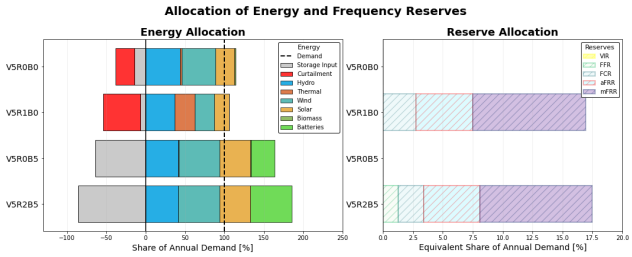

(e) Scenario 5

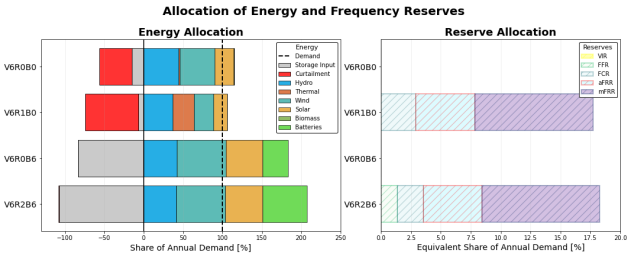

(f) Scenario 6

Figure 7: Energy and Reserve Allocation for different scenarios of simulation.

approach preserves tractability and aligns with standard center-of-inertia models, it abstracts spatial dynamics and inter-area effects. The framework therefore provides system-wide requirements that are consistent at the aggregate level, while offering a structured basis for extensions toward multi-area representations. The interaction between FRAM and UCED is formulated sequentially, allowing dynamic requirements to inform operational decisions while maintaining computational efficiency. This structure provides a practical balance between model fidelity and tractability and can be extended toward iterative implementations to further align contingency definitions with dispatch outcomes. From a computational standpoint, the framework remains tractable for large-scale UCED applications. The UCED problem is solved in approximately 45 minutes per scenario, while the FRAM module requires on the order of 3 hours due to repeated contingency evaluations. In its current implementation, N-1 security is assessed at each time step, resulting in up to 8760 contingency evaluations for a yearly simulation. In practice, many of these evaluations correspond to recurrent system conditions and can be grouped, reducing the effective computational burden. Moreover, as individual contingency assessments are independent, the FRAM stage is naturally parallelizable, enabling significant reductions in wall-clock time. The proposed structure provides a computationally efficient formulation that can be extended to larger systems and longer time horizons, while preserving a consistent representation of frequency services within operational planning. Overall, the results show that neglecting IBR-based frequency services leads to conservative operation with measurable economic and environmental penalties, whereas their explicit representation enables more efficient dispatch and improved renewable integration. The proposed framework provides a structured basis for frequency-constrained operational analysis and supports the integration of advanced control representations, including non-linear droop behavior, frequency deadbands, and damping effects in synthetic inertia.

NOMENCLATURE

Abbreviations

UCED	Unit Commitment and Economic Dispatch	mFRR	Manual Frequency Restoration Reserve
FRAM	Frequency Response Assesment Model	PFSOL	Post-fault Safe Operational Limits
VRE	Variable Renewable Energy	RoCoF	Rate of Change of Frequency
BESS	Battery Energy Storage Systems	TSO	Transmission System Operator
SIR	System Inertia Response	CE	Central Zone
VIR	Virtual Inertia Reserve	OR	Oriental Zone
FFR	Fast Frequency Reserve	NO	North Zone
FCR	Frequency Containment Reserve	SU	South Zone
aFRR	Automatic Frequency Restoration Reserve	IBR	Inverter Based Resources

FRAM Symbols

RoCoF	Rate of Change of Frequency, Hz/s or pu	Δf_{COI}	frequency deviation, Hz
fnadir	Frequency nadir, Hz	P_{CTG}	contingency, MW
H^{TOT}	total system inertia time constant, GW·s	P_{VIR}	VIR reserved power , MW
H^{SIR}	synchronous inertia , GW·s	P_{FFR}	FFR reserved power, MW
H^{VIR}	virtual inertia , GW·s	P_{FCR}	FCR reserved power , MW
τ_{VI}	delay for VIR response time, s;	P_{aFRR}	aFRR reserved power , MW
$\Delta fssmax$	Freq. at the steady state, Hz	P_{mFRR}	mFRR reserved power , MW
f_0	rated system frequency, Hz		

UCED Symbols

i	Time step in the optimization horizon	cu	Conventional units only
t	Time step in the power-swing solution	ba	Batteries only

REFERENCES

[1] Dlzar Al Kez et al. “Overview of frequency control techniques in power systems with high inverter-based resources: Challenges and mitigation measures”. en. In: *IET Smart Grid* 6.5 (2023). _eprint: https://ietresearch.onlinelibrary.wiley.com/doi/pdf/10.1049/stg2.12117, pp. 447–469. ISSN: 2515-2947. DOI: 10.1049/stg2.12117. URL: https://onlinelibrary.wiley.com/doi/abs/10.1049/stg2.12117 (visited on 03/18/2026).

[2] Ningchao Gao et al. “Developing Frequency Stability Constraint for Unit Commitment Problem Considering High Penetration of Renewables”. en. In: *2023 IEEE 50th Photovoltaic Specialists Conference (PVSC)*. San Juan, PR, USA: IEEE, June 2023, pp. 1–4. ISBN: 978-1-6654-6059-0. DOI: 10.1109/PVSC48320.2023.10360076. URL: https://ieeexplore.ieee.org/document/10360076/ (visited on 03/23/2026).

[3] Julia Matevosyan. “Survey of Grid-Forming Inverter Applications”. en. In: ().

[4] Nabil Mohammed et al. “Grid-Forming Inverters: A Comparative Study of Different Control Strategies in Frequency and Time Domains”. In: *IEEE Open Journal of the Industrial Electronics Society* 5 (2024), pp. 185–214. ISSN: 2644-1284. DOI: 10.1109/OJIES.2024.3371985. URL: https://ieeexplore.ieee.org/document/10457945/ (visited on 03/23/2026).

[5] Akhilesh Panwar et al. “RoCoF Constraint Learning Approach for Unit Commitment of Low Inertia Power System”. In: *2025 IEEE Power & Energy Society General Meeting (PESGM)*. ISSN: 1944-9933. July 2025, pp. 1–5. DOI: 10.1109/PESGM52009.2025.11225088. URL: https://ieeexplore.ieee.org/document/11225088/ (visited on 03/23/2026).

[6] Buxin She et al. “Virtual Inertia Scheduling in Unit Commitment for IBR-Penetrated Low-Inertia Systems”. In: *2025 IEEE Power & Energy Society General Meeting (PESGM)*. July 2025, pp. 1–5. DOI: 10.1109/PESGM52009.2025.11225851. URL: https://ieeexplore.ieee.org/abstract/document/11225851 (visited on 03/12/2026).

[7] Ujjwol Tamrakar et al. “Virtual Inertia: Current Trends and Future Directions”. en. In: *Applied Sciences* 7.7 (June 2017). ISSN: 2076-3417. DOI: 10.3390/app7070654. URL: https://www.mdpi.com/2076-3417/7/7/654 (visited on 03/12/2026).

[8] Yuting Teng et al. “Review on grid-forming converter control methods in high-proportion renewable energy power systems”. In: *Global Energy Interconnection* 5.3 (June 2022), pp. 328–342. ISSN: 2096-5117. DOI: 10.1016/j.gloei.2022.06.010. URL: https://www.sciencedirect.com/science/article/pii/S2096511722000640 (visited on 03/18/2026).

[9] Honglei Xu et al. “Frequency-Constrained Robust Unit Commitment Model Considering Virtual Inertia Control of Wind Farms”. In: *2024 IEEE PES 16th Asia-Pacific Power and Energy Engineering Conference (APPEEC)*. Oct. 2024, pp. 1–5. DOI: 10.1109/APPEEC61255.2024.10922577. URL: https://ieeexplore.ieee.org/abstract/document/10922577 (visited on 03/12/2026).

[10] Jing Ye et al. “Unit commitment in isolated grid considering dynamic frequency constraint”. In: *2016 IEEE Power and Energy Society General Meeting (PESGM)*. ISSN: 1944-9933. July 2016, pp. 1–5. DOI: 10.1109/PESGM.2016.7741654. URL: https://ieeexplore.ieee.org/abstract/document/7741654 (visited on 03/19/2026).

ACKNOWLEDGEMENT

The authors gratefully acknowledge the financial support and resources provided by the ARES-CDD and ARES PRDBOL2022 programmes, which were instrumental in the successful completion of this work.